Eur. Phys. J. D **18**, 83–86 (2002)
DOI: 10.1140/e10053-002-0010-y

THE EUROPEAN PHYSICAL JOURNAL D
EDP Sciences

Lowest breathing mode of bosonic helium clusters

D. Blume[a] and Chris H. Greene

JILA and Department of Physics, University of Colorado, Boulder, CO 80309-0440, USA

Received 11 July 2001

Abstract. We analyze various microscopic calculations of vibrational frequencies for ^4He_N clusters, $N = 3$–728. The lowest breathing frequency with total angular momentum $J = 0$ varies smoothly as a function of N, with a maximum around $N = 50$–120.

PACS. 36.40.-c Atomic and molecular clusters – 67.40.Db Quantum statistical theory; ground state, elementary excitations – 67.40.-w Boson degeneracy and superfluidity of ^{4}He

The calculation of excited state properties of many-body systems is intrinsically more challenging than that of ground state properties. However, only excited state properties are directly accessible experimentally and allow a straightforward comparison between theory and experiment. The determination of excitation frequencies of liquid bulk ^{4}He, two-dimensional ^{4}He films and finite size ^4He_N clusters has long been an area of active research. This is primarily because excitations such as phonons, rotons and vortices are a direct signature of superfluidity. The superfluid phase of bulk ^{4}He (Refs. [1,2] and references therein) and ^{4}He films [3–7] has been studied extensively since the 1930s and 1970s, respectively. The study of superfluidity of ^4He_N clusters, in contrast, started more recently. Superfluidity of these finite size bosonic clusters with more than $N \approx 60$ atoms has been established theoretically in 1989/90 [8,9], and six years later experimentally [10,11]. (We omit the mass number (4) in the following, and refer to ^{4}He as He.)

This paper focuses on the lowest vibrational frequency (breathing/bulk mode) of bosonic He_N clusters, which has been estimated in the literature using various microscopic approximations [12–16]. These microscopic quantum mechanical studies of the lowest breathing mode of He_N clusters with $N = 3$–728 have been performed using an adiabatic approximation [12], an excitation operator approach [13–15], and a random phase approximation with a phenomenological effective interaction [16]. Some of these studies are based on solving the many-body Hamiltonian at zero temperature by writing the many-body potential surface as a sum of two-body atom-atom potentials. The microscopic frequency studies summarized in this paper use a variety of different two-body potentials since the He–He two-body potential has been "fine-tuned" repeatedly, mostly by Aziz and coworkers [17–19]. However, small differences of the energetics due to the usage of different two-body potentials are irrelevant for our purposes in this paper.

The adiabatic approximation [12] treated He_N clusters with up to $N = 10$ atoms, and only recently narrowed the gap between "exact" basis set expansion calculations for the trimer [20,21] and calculations for the larger clusters with $N = 20$–728 [13–16]. A classical liquid drop model [22] has been applied to even larger clusters, connecting the lowest breathing mode of finite He_N clusters with that of bulk He. We find that the compressional excitation frequency $\hbar\omega_0 = E_1 - E_0$ as a function of the number of atoms N in the cluster follows a smooth behavior. $\hbar\omega_0$ is small in the small and large N limit, and shows a distinct maximum around $N = 50$–120.

Figures 1 and 2 summarize the absolute value of the ground state energy per particle, $|E_0/N|$, together with the absolute value of the chemical potential, $|\mu|$, and the lowest vibrational frequency, $\hbar\omega_0 = E_1 - E_0$, as a function of the number of atoms N in the cluster. Figure 1 shows these data, which are taken from various publications [12–16,23–25], on a linear N scale ($N = 3$–100), whereas Figure 2 shows the same data on a $N^{-1/3}$ scale ($N \geq 3$). First, consider the absolute value of the ground state energy per particle, $|E_0/N|$. E_0/N can be calculated efficiently *via* the diffusion Monte Carlo method, which calculates the many-body ground state for a given potential surface "essentially exactly" [26]. In many problems, the variational Monte Carlo method is adequate; it minimizes the ground state energy for some assumed functional form of the many-body wave function [26]. For the larger clusters, the ground state energy per particle, E_0/N, can be fitted to high accuracy with a liquid drop formula containing a volume, a surface and a curvature term, $E_0/N = E_v + E_s x + E_c x^2$, where $x = N^{-1/3}$ [15,22, 23]. It is this $N^{-1/3}$ dependence that motivates our scale of the abscissa in Figure 2.

[a] e-mail: doerte@wsu.edu
Present address: Department of Physics, Washington State University, Pullman, WA 99164-2814, USA.

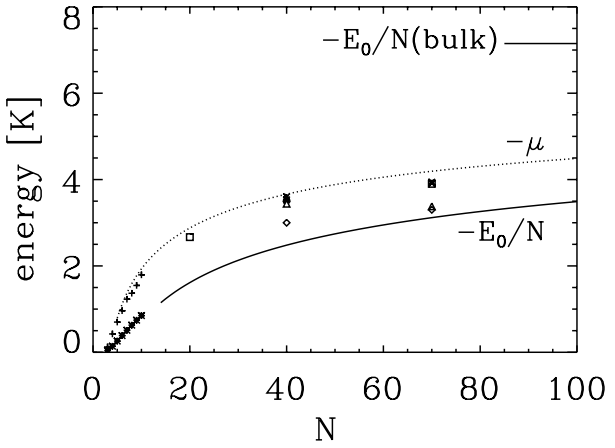

Fig. 1. Absolute value of the ground state energy per particle, $|E_0/N|$, together with the absolute value of the chemical potential, $|\mu|$, and the lowest breathing mode $\hbar\omega_0$ of He_N clusters as a function of N. The data are collected from various publications. Asterisks and a solid line indicate $|E_0/N|$, and a dotted line indicates $|\mu|$ [12,15,22]. The plus symbols show the excitation energies calculated *via* an adiabatic approximation [12], the squares and triangles show energies calculated *via* an excitation operator approach combined with the variational Monte Carlo method [13–15], while the crosses depict calculations based on an excitation operator approach combined with the diffusion Monte Carlo method [14,15]. The absolute value of the ground state energy per particle for liquid bulk He, $|E_0(\text{bulk})/N|$, is indicated on the upper right corner by a solid horizontal line.

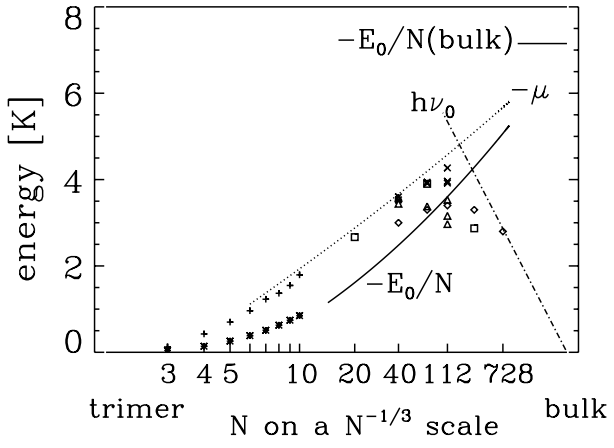

Fig. 2. Absolute value of the ground state energy per particle, $|E_0/N|$, together with the absolute value of the chemical potential, $|\mu|$, and the lowest breathing mode $\hbar\omega_0$ of He_N clusters as a function of N (on a $N^{-1/3}$ scale). These data are also shown in Figure 1 for $N \leq 100$ (see caption of Fig. 1 for legend of symbols). Additionally, diamonds show $\hbar\omega_0$ calculated *via* a random phase approximation with an effective phenomenological interaction [16], and a dashed-dotted line calculated *via* a classical liquid drop model [15,22].

Both figures, Figures 1 and 2, show the absolute value of the resulting diffusion Monte Carlo ground state energies per particle, $|E_0/N|$, by asterisks for $N = 3$–10 [12]. For the larger clusters, we plot a fit to the liquid drop formula rather than the many-body ground state energies themselves (solid line) [15]. For comparison, a horizontal solid line in the upper right corner indicates the absolute value of the ground state energy per particle of bulk liquid He, $|E_0/N(\text{bulk})| = 7.15$ K. The absolute value of the ground state energy per particle of bulk He is significantly larger than that of the $N = 728$ cluster, indicating that the energetics of clusters this large are still affected by edge effects. In addition to $|E_0/N|$, Figures 1 and 2 also show the absolute value of the chemical potential, $|\mu|$, defined as the energy difference of a cluster with N and $N-1$ atoms, $\mu = E_0(N) - E_0(N-1)$, and calculated using the liquid drop formula (dotted line).

Now consider the microscopic excitation frequency calculations, which can be divided into three groups; the adiabatic hyperspherical approximation ($N = 3$–10) [12], the excitation operator ansatz ($N = 20$–240) [13–15], and the random phase approximation with a phenomenological effective interaction ($N = 40$–728) [16]. The key point of the adiabatic approximation [27] (and references therein) is the identification of an overall coordinate, the hyperspherical radius R, where $R^2 \propto \sum_i (\mathbf{r}_i - \mathbf{r}_{\text{cm}})^2$. Here, $\mathbf{r}_i$ denotes the Cartesian position vector of atom i, and $\mathbf{r}_{\text{cm}}$ the center-of-mass vector of the cluster. Averaging over all degrees of freedom except for the hyperspherical radius coordinate R results in an effective one-dimensional potential curve along R. The first excited state in this potential curve then corresponds to the lowest breathing mode of excitations. In its simplest implementation, the adiabatic approximation neglects coupling between angular and radial degrees of freedom. Previous work has shown, however, that it is important for an appropriate description of He_N clusters to include a diagonal coupling element (see Ref. [12] for a detailed discussion). Figures 1 and 2 show the results of this study, including the diagonal coupling element in an appropriate manner, for $N = 3$–10 (pluses).

The basic idea of the second set of calculations [13–15], namely the excitation operator approach, differs significantly from the adiabatic approximation. In analogy to the treatment of excitations in bulk He, the excitation operator approach is based on a Feynman ansatz [28] for the excited state wave function ψ_{F}, namely ψ_{F} is written as a product of the ground state wave function ψ_0 and an excitation operator F, where $F = \sum_i f(\mathbf{r}_i - \mathbf{r}_{\text{cm}})$. This ansatz allows one to calculate the excitation energies directly from the ground state static structure function of the cluster by solving a generalized Feynman eigenvalue problem *via* ground state Monte Carlo techniques [13–15].

Two research groups followed this approach. Rama Krishna and Whaley [13] determined the He cluster ground state densities using variational Monte Carlo methods, and Chin and Krotscheck [14,15] using variational and diffusion Monte Carlo methods. The variational Monte Carlo calculation uses an energy optimized trial wave function, and the extracted structural properties can therefore be biased. The diffusion Monte Carlo calculation, in contrast, is limited only by the statistical and extrapolation errors in sampling the exact one- and

two-body ground state densities entering into the static structure function. Figures 1 and 2 show the results based on a variational Monte Carlo calculation (squares [13] and triangles [14,15]), and based on diffusion Monte Carlo calculations (crosses [14,15]). The overall agreement between these calculations is reasonable, although, discrepancies of up to 30% exist. These discrepancies are not surprising, given that the calculations are performed for various different trial wave functions, and since they utilize different minimization and/or orthogonalization schemes [13–15].

Now consider the third set of microscopic calculations of the lowest breathing mode, the random phase approximation calculations [16]. Casas and Stringari solve the random phase approximation equations for a phenomenological effective interaction using an energy functional, whose parameters are determined so that the experimental values for the binding energy, saturation density, compressibility parameter, and surface tension of bulk liquid ^{4}He at saturation and zero temperature are reproduced [29]. Then, the effective interaction depends on one coordinate only, thereby reducing the numerical complexity of the random phase equations enormously. Interestingly, it is convenient to solve the random phase approximation equations by calculating a response function corresponding to a given excitation operator F. For the symmetric compressional mode, reference [16] chooses $F = \sum_i f(\mathbf{r}_i)$, where $f(\mathbf{r}_i) = r_i^2$. This excitation operator F is proportional to the squared hyperradius R introduced above, except for a center-of-mass offset that we believe should be negligible in this case. Figures 1 and 2 summarize the results of this study (diamonds).

For large clusters, $N \geq 500$, the lowest breathing mode frequency can be estimated reliably within a classical liquid drop model [22]. Within this model, $\hbar\omega_0$ is given by the phonon dispersion relation $\hbar\omega_0 = ck$. c denotes the velocity of sound, $c = 238$ m/s, whereas k is fixed through a boundary condition imposed by the requirement that excess pressure cannot be maintained at a free surface, $j_0(kr_c) = 0$. Here, j_0 denotes the lowest order Bessel function, and $r_c = r_0 N^{1/3}$ the radius of the cluster, where $r_0 = 2.22$ Å [25]. The lowest breathing mode is then given by $\hbar\omega_0 = 25.6 N^{-1/3}$ K [15]. Figure 2 shows this prediction as a dashed-dotted line for $N \geq 100$.

In summary, the excitation frequency $\hbar\omega_0$ of the lowest breathing mode calculated *via* the adiabatic approximation for $N = 3$ [20,30] agrees well with that from a coupled channel calculation [20,21]. The frequency for the clusters with $N \leq 10$ calculated *via* the adiabatic approximation [12] connect smoothly with the frequency for the $N = 20$ cluster calculated *via* the excitation operator approach [13]. While $\hbar\omega_0$ increases monotonically with increasing N for $N \leq 40$, this quantity shows some scattering around $N = 40$–240 (see also discussion above). A maximum around $N = 50$–120, however, is clearly recognizable. The frequencies for the $N = 112$ and $N = 240$ cluster calculated based on the excitation operator ansatz [13–15] agree to better than 20% with the frequencies calculated based on the random phase approximation with an effective phenomenological interaction [16]. Furthermore, the random phase approximation frequency of the largest cluster treated, $N = 728$, almost coincides with that predicted by the classical liquid drop model [22], which gives a good description for clusters with $N \geq 500$. In short, the lowest breathing mode frequency of He_N clusters is small in both the small and large N limits, and exhibits a maximum around $N = 50$–120.

The calculated values of $\hbar\omega_0$ shown in Figures 1 and 2 are not new (see above, and also [15]). However, the very recent calculations for small He_N clusters, $N \leq 10$ [12], help to complete the picture that had emerged from the earlier calculations, in that the breathing mode has now been calculated for the whole range of cluster sizes, namely from the He trimer to bulk He.

Chin and Krotscheck [15] interpreted the behavior of $\hbar\omega_0$ as a function of N through the classical liquid drop model equation $\hbar\omega_0 = ck$, as follows. For small N, the interior density of a cluster increases as a function of N, and therefore also the compressibility $b_{\rm comp}$ and the speed of sound c, $c = \sqrt{b_{\rm comp}/m}$ [22] (m, mass of He atom). Even though k decreases with increasing N, overall the increase in c is larger than the decrease in k, leading to an increase of the breathing excitation frequency with increasing N (for $N \leq 50$–120). For large N, $N \geq 112$, the interior density is approximately constant [23], as are also $b_{\rm comp}$ and c, to lowest order. An increase in cluster size then leads to a decrease of the wave vector k of the excitation, and therefore to an decrease of the breathing excitation.

Note that the "turn-around" region of the $\hbar\omega_0$ curve, around $N = 50$–120, coincides with the onset of superfluidity of He_N clusters, $N \approx 60$. We can now ask whether a connection exists between the studies summarized here and the superfluid nature of He clusters with more than $N = 60$ atoms, *i.e.*, their phonon-roton dispersion curve. To begin with, recall that the roton minimum of bulk He occurs at a wave length $k = 1.93$ Å^{-1} with energy $E = 8.65$ K. This minimum roton energy is somewhat larger than the heat of evaporation, $-E_0/N(\text{bulk}) = 7.15$ K, and the roton evidently has metastable character. We speculate that the roton of a bosonic He_N cluster with about $N \geq 60$ may be described within the adiabatic approximation by a higher lying adiabatic potential curve with total angular momentum $J = 0$, which describes an excitation of two small rotating subunits, each with some nonzero internal angular momentum j (see also Ref. [31]). In this picture, the metastability could arise from an avoided crossing between the lowest $J = 0$ potential curve and one or more excited $J = 0$ potential curves, or from a potential barrier of a $J = 0$ potential curve, which separates the "roton state" from a second minimum at smaller hyperradius R. This qualitative picture seems to be in agreement with recent calculations of the velocity field in the region of the roton minimum for bulk He [32,33]. However, more calculations are needed to refine and test these ideas in detail.

This work was supported partly by the National Science Foundation. D. B. acknowledges support through a DFG Postdoktorandenstipendium.

References

1. D.R. Tilley, J. Tilley, *Superfluidity and Superconductivity*, 3rd edn. (Hilger, Bristol, New York, 1990).
2. H.R. Glyde, *Excitations in Liquid and Solid Helium* (Clarendon Press, Oxford, 1994).
3. J.M. Kosterlitz, D.J. Thouless, J. Phys. C **6**, 1181 (1973).
4. D.R. Nelson, J.M. Kosterlitz, Phys. Rev. Lett. **39**, 1201 (1977).
5. D.J. Bishop, J.D. Reppy, Phys. Rev. Lett. **40**, 1727 (1978).
6. I. Rudnick, Phys. Rev. Lett. **40**, 1454 (1978).
7. D. McQueeney, G. Agnolet, J.D. Reppy, Phys. Rev. Lett. **52**, 1325 (1984).
8. P. Sindzingre, M.L. Klein, D.M. Ceperley, Phys. Rev. Lett. **63**, 1601 (1989).
9. M.V. Rama Krishna, K.B. Whaley, Phys. Rev. Lett. **64**, 1126 (1990).
10. M. Hartmann, F. Mielke, J.P. Toennies, A.F. Vilesov, G. Benedek, Phys. Rev. Lett. **76**, 4560 (1996).
11. S. Grebenev, J.P. Toennies, A.F. Vilesov, Science **279**, 2083 (1998).
12. D. Blume, C.H. Greene, J. Chem. Phys. **112**, 8053 (2000).
13. M.V. Rama Krishna, K.B. Whaley, J. Chem. Phys. **93**, 6738 (1990).
14. S.A. Chin, E. Krotscheck, Phys. Rev. Lett. **65**, 2658 (1990).
15. S.A. Chin, E. Krotscheck, Phys. Rev. B **45**, 852 (1992).
16. M. Casas, S. Stringari, J. Low Temp. Phys. **79**, 135 (1990).
17. R.A. Aziz, V.P.S. Nain, J.S. Carley, W.L. Taylor, G.T. McConville, J. Chem. Phys. **70**, 4330 (1979).
18. R.A. Aziz, F.R.W. McCourt, C.C.K. Wong, Mol. Phys. **61**, 1487 (1987).
19. R.A. Aziz, M.J. Slaman, J. Chem. Phys. **94**, 8047 (1991).
20. E. Nielsen, D.V. Fedorov, A.S. Jensen, J. Phys. B **31**, 4085 (1998).
21. D. Blume, C.H. Greene, B.D. Esry, J. Chem. Phys. **113**, 2145 (2000).
22. A. Bohr, B.R. Mottelson, *Nuclear Structure*, (W.A. Benjamin, Inc., Reading, 1975), Vol. II.
23. V.R. Pandharipande, J.G. Zabolitzky, S.C. Pieper, R.B. Wiringa, U. Helmbrecht, Phys. Rev. Lett. **50**, 1676 (1983).
24. S.C. Pieper, R.B. Wiringa, V.R. Pandharipande, Phys. Rev. B **32**, 3341 (1985).
25. V.R. Pandharipande, S.C. Pieper, R.B. Wiringa, Phys. Rev. B **34**, 4571 (1986).
26. B.L. Hammond, W.A. Lester Jr, P.J. Reynolds, *Monte Carlo Methods in Ab Initio Quantum Chemistry* (World Scientific, Singapore, 1994).
27. C.D. Lin, Phys. Rep. **257**, 1 (1995).
28. R.P. Feynman, Phys. Rev. **94**, 262 (1954).
29. S. Stringari, J. Treiner, J. Chem. Phys. **87**, 5021 (1987).
30. B.D. Esry, C.D. Lin, C.H. Greene, Phys. Rev. A **54**, 394 (1996).
31. V.I. Kruglov, M.J. Collett, Phys. Rev. Lett. **87**, 185302 (2001).
32. D.E. Galli, E. Cecchetti, L. Reatto, Phys. Rev. Lett. **77**, 5401 (1996).
33. L. Reatto, D.E. Galli, Int. J. Mod. Phys. B **13**, 607 (1999).